

**Damian Janiga*, Robert Czarnota*,
Jerzy Stopa*, Paweł Wojnarowski***

MICROSCALE MODELING OF CO₂-EOR PROCESS IN COUPLING WITH LABORATORY MEASUREMENTS**

1. INTRODUCTION AND DECISION FRAMEWORK

Among oil reservoir production technique approximately one third reservoirs are recovered by primary method [2]. Several Improve Oil Recovery (IOR) and Enhanced Oil Recovery (EOR) techniques exist to increase the recovery of oil from reservoir. Improved oil recovery strategies include studies of multiphase fluid flow mechanisms, reservoir description and modeling, development of smarter drilling techniques and injection of various types of liquids containing polymers, surfactants, enzymes and foam, gas injection and WAG. Gas injection method can be effectively used in worldwide oil fields, but due to geological and technological condition some presumptions need to be done [6]. Foreign experience cannot be directly transferred to national oil fields before proceeding number of laboratory experiments, numerical simulations and pilot tests [10]. As the technology and the tools for modeling and simulating the multiphase fluid flow in the reservoirs are rapidly developing, the need for high quality and preferably in situ input data is increasing [3]. Important quantities of reservoir physics including porosity, absolute and relative permeability can affect production potentials. In presented paper effort was made to develop and test decision framework (Fig. 1), combining laboratory core flood experiment with numerical simulation.

* AGH University of Science and Technology, Faculty of Drilling, Oil and Gas, Krakow, Poland

** Paper prepared within the statutory research program of the Faculty of Drilling, Oil and Gas, AGH University of Science and Technology No. 11.11.190.555

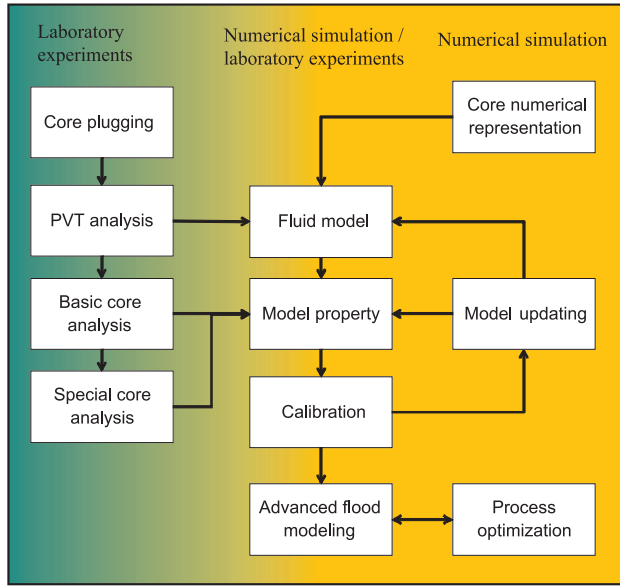


Fig. 1. Decision framework for combination of laboratory experiment and numerical simulation

2. MATERIALS AND METHODS FOR LABORATORY EXPERIMENT

2.1. PVT characteristic of oil

For binary brine – oil flood experiment, crude oil from one of polish fields was selected. Density and viscosity was determined according to ASTM D1480-15 and ISO 12058-1 standards respectively. Structural group and fractional composition were performed on PN-72/C-04025 and ISO 2285 procedures. Results of PVT characteristic are presented in Table 1 and Figure 2. A complete crude oil properties summary was reported in the previous author’s investigation [5].

Table 1
Physical properties of crude oil

Density [kg/m ³]	Gravity [°API]	Water content [%]
827 (23°C)	39.6 (23°C)	0.18
Viscosity [cP]	Temperature [°C]	
5.50	20	
4.27	30	
3.37	40	
2.87	50	
2.48	60	

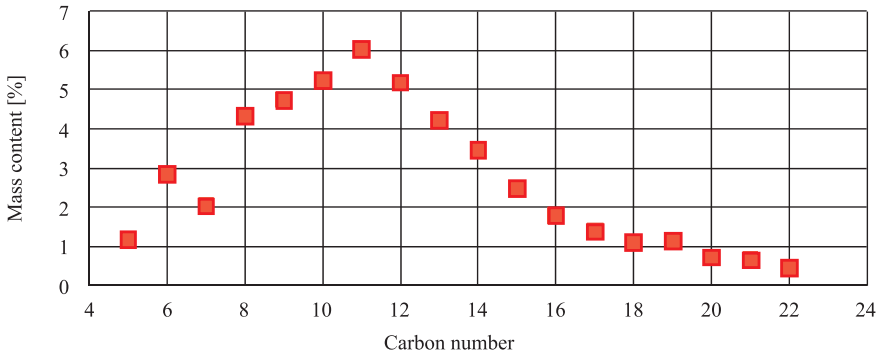


Fig. 2. The content of individual fraction expressed as a percentage by mass

2.2. Core flood apparatus

Experimental facility (AFS-300 Core Lab) used for relative permeability determination consist of:

- four Teledyne Isco synergine pumps for controlling overburden, pore and back pressure,
- two piston type accumulators for experimental fluids connected to the pumps,
- core holder for 1.5” sample diameter,
- acoustically monitored separator (AMS),
- backpressure regulator (BPR),

as is shown in Figure 3.

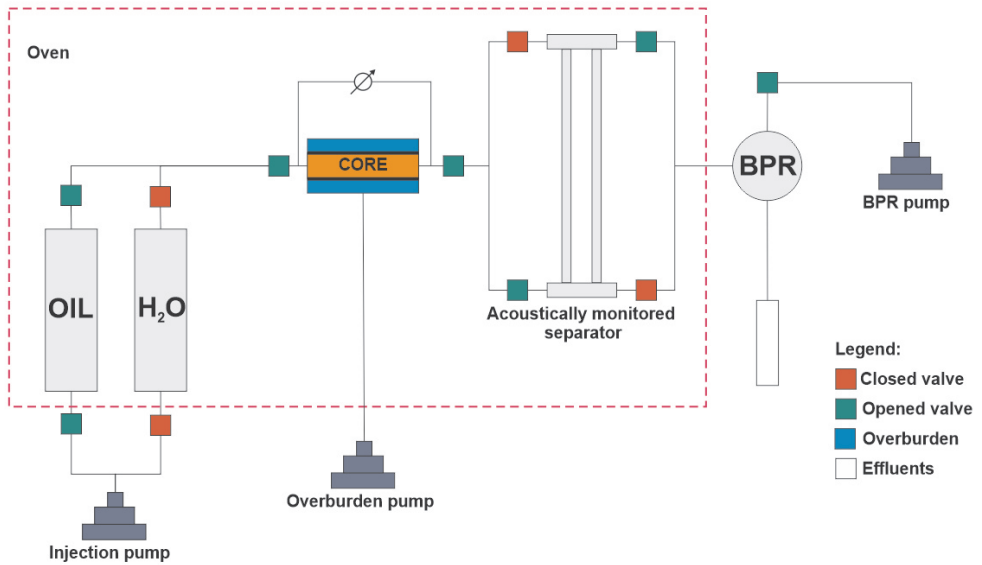


Fig. 3. Experimental facility for determination of relative permeability

The outlet fluid flow line was connected to an acoustic separator and through it to a backpressure regulator (BPR). Acoustic separator is a device equipped with an ultrasonic transducer for interface detection of two different immiscible phases (liquid/liquid, gas/liquid). Differential pressure sensor was installed for registration pressure differences during measurement.

2.3. Rock samples and routine core analysis

Core flood experiments were performed on sandstone rock sample collected from Outer Eastern Carpathians outcrop, transported to workshop for drilling and saw cutting. As a result cylindrical shape of rock plug was obtained for further investigation. Porosity and absolute permeability were performed for sample noted as C10. Porosity and core sample pore volume were determined from mass balance method which is based on bulk volume, mass of dry and fully saturated with distilled water plug. Absolute permeability was measured at room condition (23°C) using nitrogen. Determined absolute permeability included Klinkenberg correction factor because of occurrence of slippage phenomenon. The C10 sample characteristic is included in Table 2.

Table 2
Characteristic of core sample

Core ID	Diameter	Length	Porosity	Absolute permeability	Pore volume	Bulk density
	[cm]	[cm]	[%]	[mD]	[cm ³]	[kg/m ³]
C10	3.75	8.34	12.18	7.63	11.22	2 272

2.4. Advanced core sample analysis

Relative permeability

The core flood experiments were conducted using C10 sample. Before the oil injection began, the cores were initially 100% saturated with synthetic reservoir brine using vacuum pump. Coreholder was assembled with analyzed sample and reservoir crude oil was injected into core with constant rate 1 ml/min. Parallel to injection process, differential pressure was measured. The quantity of effluents was registered by acoustically monitored separator in experimental conditions, and with electronic balance at room conditions. By analyzing differential pressure and effluents volume during experiment, relative permeability for oil – water system can be obtained using unsteady state method. Total water production and pressure drop during flooding experiment are presented in Figure 4.

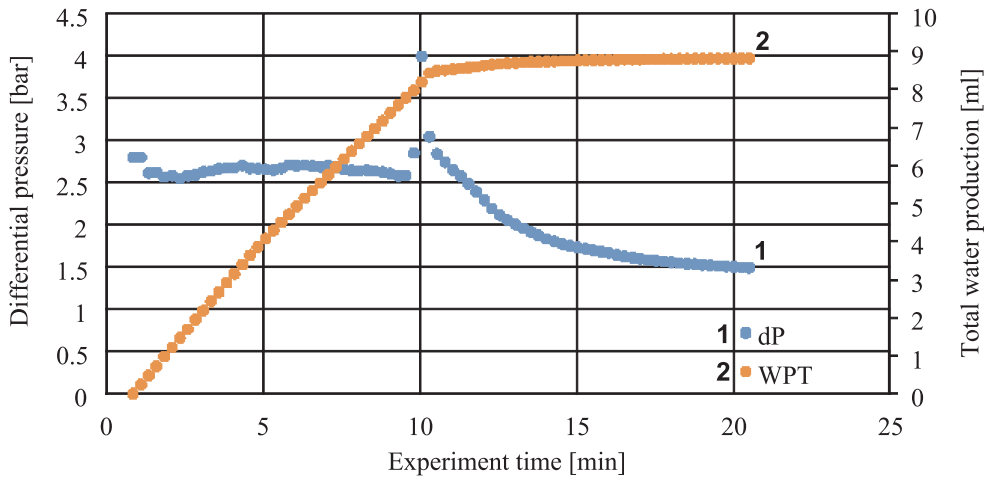


Fig. 4. Changing of differential pressure (dP) and total water production (WPT) during oil injection into C10 core sample

After 10.5 min of experiment, oil breakthrough is observed in opposite side of core. Breakthrough time is also noticeable in pressure plot at 4 bar of difference pressure, after that pressure evenly dropped to 1.5 bar after 21 minutes of experiment. Average water saturation after oil flood is 21.42%, which can be described as initial water saturation (Sw_i). Directly measured pressure change and water production were analyzed in Cydar, which is sophisticated SCAL (special core analysis) software. Results of relative permeabilities for brine – oil system were obtained and are presented in Figure 5.

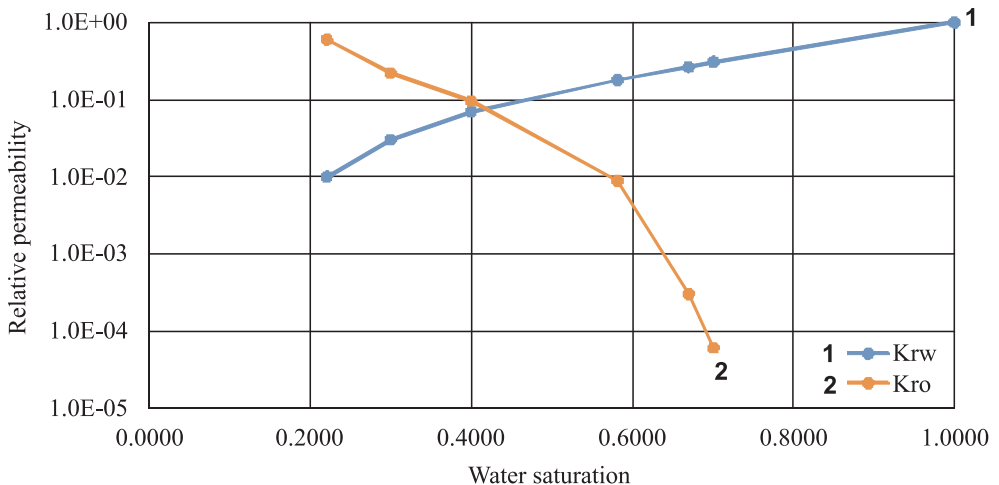


Fig. 5. Relative permeability curves for oil (Kro) and water (Krw) obtained for flood experiment

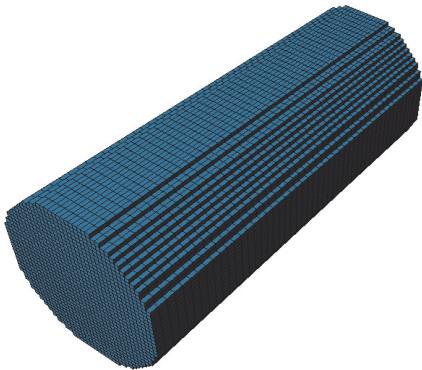
Shapes of curves are characteristic for water wet reservoir, which are related to previous authors investigation [4]. Experiment related to oil injection into brine-filled core can be considered as primary or secondary hydrocarbon migration process [9].

3. CORE FLOOD NUMERICAL SIMULATION

Numerical model calibration

Core sample geometry, porosity and permeability were reconstructed in numerical reservoir simulator, by discretization in 76 050 cells ($50 \times 39 \times 39$). Model and physical representation of sample C_{10} is presented in Figure 6. Due to the impossibility of pore space imaging, core model is homogenous and isotropic with average porosity and permeability 12.18% and 7.63 mD, respectively. Model was created in Eclipse E300 software using laboratory units. Numerical model of C_{10} sample have 11.42 ml of pore volume what is 1.7% difference in laboratory measurements.

a)



b)



Fig. 6. Numerical model of C_{10} sample (a) and core sample (b)

Calibration of proposed numerical core model based on laboratory experiment including brine – oil relative permeability is presented in Figure 7. Mean square error of pressure calibration is 0.05 bar^2 and for total water production is less than 0.001 ml^2 .

For gas – oil flow relative permeability was generated with Corey analytical model. Changes of oil saturation during calibration process are presented in Figure 8, after 1 and 5 minutes of oil injection.

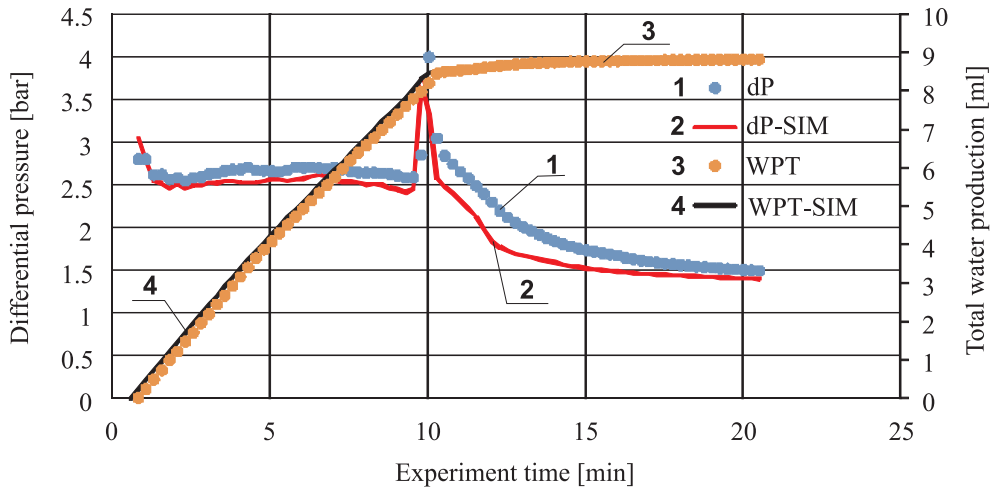


Fig. 7. Core numerical model calibration to laboratory experiment

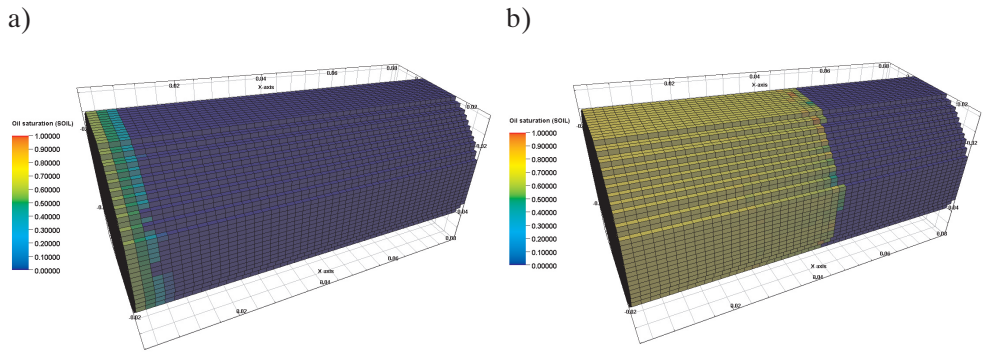


Fig. 8. Oil flooding profile after 1 minute of injection (a) and after 5 minute (b) during numerical model calibration

CO₂ – flood modeling

Effect of CO₂ injection rates are investigated for three different flooding scenarios: 0.5, 1 and 2 ml/min. Efficiency was determined by comparison the total oil production after 158 minutes of CO₂ injection. Decreasing injection rate from 1 ml/min to 0.5 ml/min affects total oil production causing 10.04% decline, on the other hand, increasing rate form 1 ml/min to 2 ml/min improves production by 9.05%. Oil production during experiment simulation is presented in Figure 9. Boost of injection rates improves flooding sweep efficiency, especially in bottom part of core sample and is presented in Figure 10.

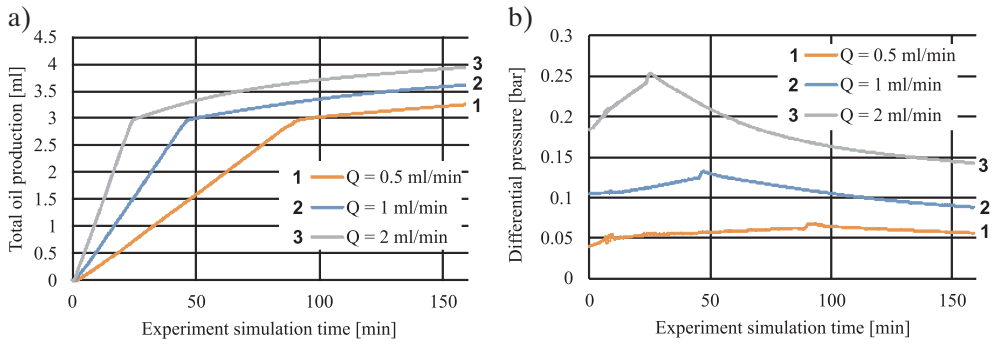


Fig. 9. Total oil production (a) and differential pressure (b) for different CO₂ injection rates, based on simulation model

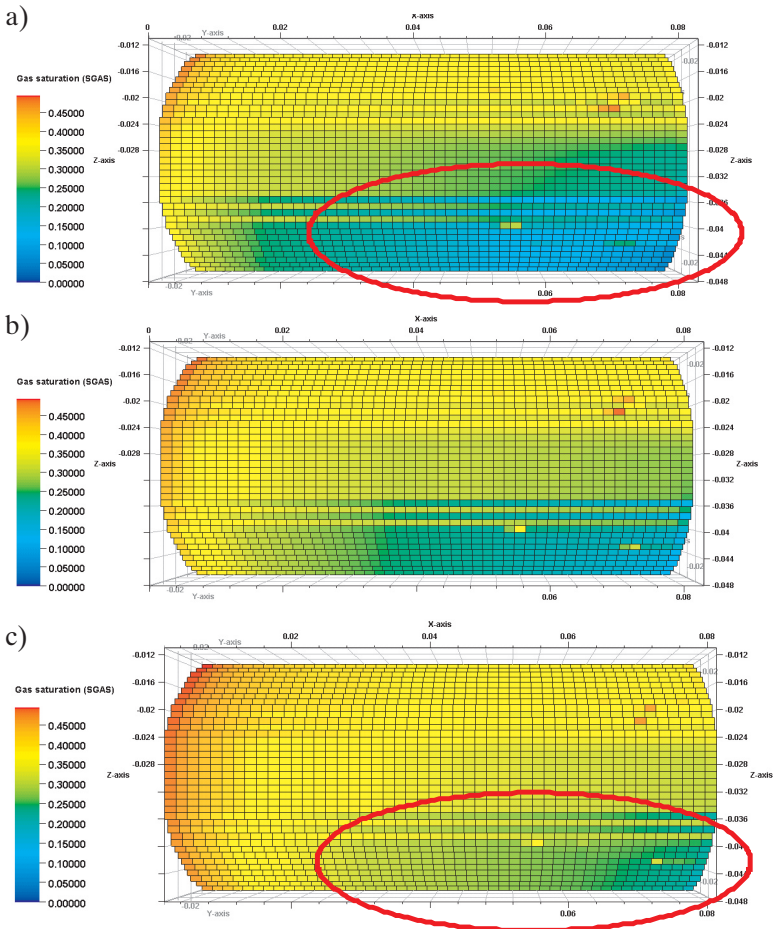


Fig. 10. CO₂ saturation after 188 minutes for CO₂ injection rates 0.5 ml/min (a), 1 ml/min (b) and 2 ml/min (c). Improved areal sweep efficiency is marked by red oval

Water alternating gas (WAG) flood modeling

For WAG process modeling two different scenarios was created, for the first injection 0.22 pore volume (PV) (2.5 ml) was flushed with water rate equal 0.1 ml/min and CO₂ injection started with rate of 2 ml/min. The second experiment assumed injection of 0.11PV of water before CO₂ flooding. Total numerical experiment time was 158 minutes, and the changes of oil and water production are presented in Figure 11. As a result of WAG flooding, total oil production is 4.6 ml for 0.22PV and 4.52 ml for 0.11PV water injection scenarios. One of major parameters of WAG effectiveness is ratio of production to injection water volume. In case of 0.22PV water injection, effectiveness is 79.52% and 67.68% for the second scenario.

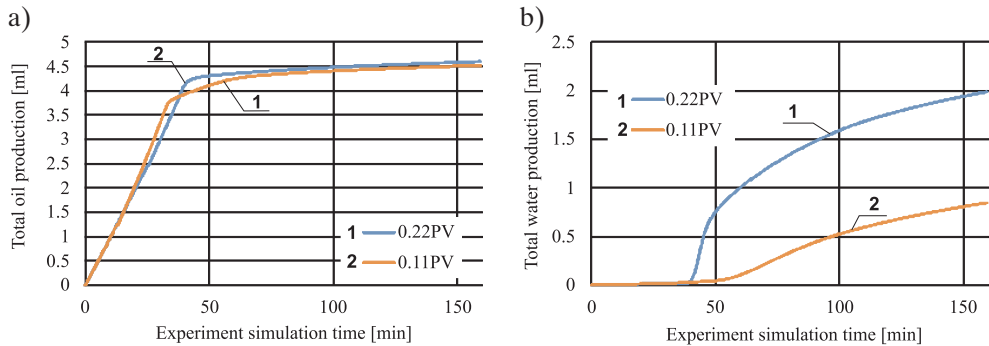


Fig. 11. Total oil production (a) and water production (b) in case of WAG flood process, based on simulation model

Water before CO₂ injection reduce mobility of gas, and as a result increase of total oil production can be observed. Changes of saturation profiles are presented in Figure 12 for injected 0.22PV of water and Figure 13 for 0.11PV respectively.

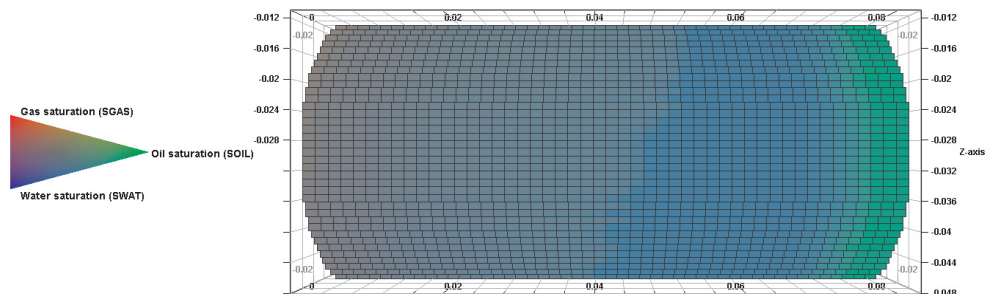


Fig. 12. Saturation profiles after 58 minutes of injection. Transition zone between oil and water is relatively stable, opposite to gas oil zone

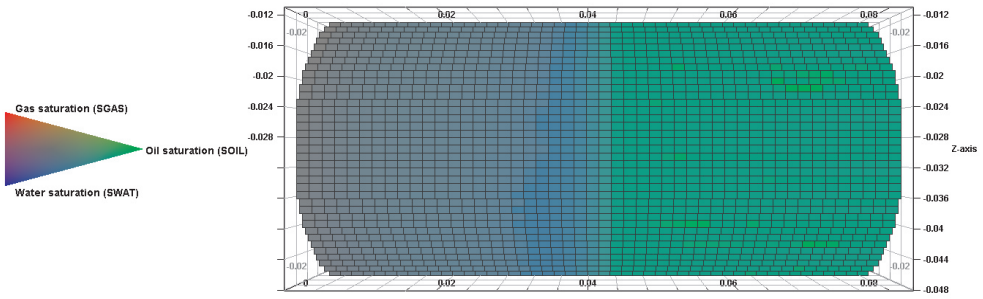


Fig. 13. Saturation profiles after 41 minutes of injection

4. CONCLUSION

Conjunction of laboratory measurements with numerical simulation can be effective tool for prediction of flooding process efficiency in case of whole range of input parameters. Precise calibration between laboratory data and numerical results is necessary for further investigation. Decision framework include basic and special core analysis for determining porosity, absolute and relative permeability. At actual level of advanced in porous space distribution description, presented framework assumes homogenous sample, but numerical model can be extended to heterogeneous by including MRI, X-Ray or other scanning technique. Obtained laboratory data are integrated with numerical representation of core sample. As an example of flowchart results, five different CO₂ injection core flood scenarios were investigated. Results of numerical simulation presented in Figure 14 reveal that the injection rate as well as WAG process have influence on oil production.

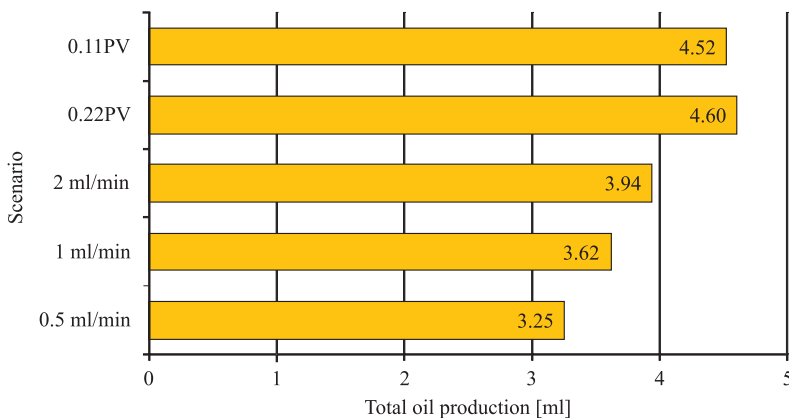


Fig. 14. A summary of numerical experiment results in case of total oil production

Numerical model can also be used for process design optimization, because micro scale of analyzed sample allows precisely to describe phenomena during flow. After upscaling, results can be transferred into full scale numerical model.

REFERENCES

- [1] ASTM D1480-15: *Standard Test Method for Density and Relative Density (Specific Gravity) of Viscous Materials by Bingham Pycnometer*. ASTM, International, West Conshohocken, PA, 2015.
- [2] Bon J.: *Laboratory and Modelling Studies on the Effects of Injection Gas Composition on CO₂-Rich Flooding in Cooper Basin*. South Australia, 2009.
- [3] Brautaset A.: *In situ fluid dynamics and CO₂ injection in porous rocks*. 2009.
- [4] Czarnota R., Janiga D., Stopa J., Wojnarowski P.: *Laboratory measurement of wettability for Ciężkowice sandstone*. AGH Drilling, Oil, Gas, vol. 33, No. 1, 2016, pp. 167–172.
- [5] Czarnota R., Janiga D., Stopa J., Wojnarowski P.: *Determination of minimum miscibility pressure for CO₂ and oil system using acoustically monitored separator*. Journal of CO₂ Utilization, 17, 2017, pp. 32–36.
- [6] Ezekwe N.: *Petroleum reservoir engineering practice*. Pearson Education, 2010.
- [7] ISO 12058-1: *Plastics – Determination of Viscosity Using a Falling-ball Viscometer*, 1997.
- [8] ISO 22854: *Liquid Petroleum Products – Determination of Hydrocarbon Types and Oxygenates in Automotive-motor Gasoline – Multidimensional Gas Chromatography Method*, 2008.
- [9] PN-72/C-04025: *Hydrocarbon Structural Group Composition Analysis by Chromatography*, 1972.
- [10] Ungerer P., Burrus J., Doligez B., Chenet P. Y., Bessis F.: *Basin Evaluation by Integrated Two-Dimensional Modeling of Heat Transfer, Fluid Flow, Hydrocarbon Generation, and Migration (1)*. AAPG Bulletin, 74(3), 1990, pp. 309–335.
- [11] Wojnarowski P.: *Potential for increasing oil recovery from Polish oil-fields by applying EOR methods* [Analiza możliwości zwiększenia efektywności wydobycia ropy naftowej z polskich złóż w oparciu o metody EOR]. Gospodarka Surowcami Mineralnymi [Mineral Resources Management], 28(4), 2012, pp. 47–58.